Detecting Longitudinal Position of Internal Log Hole Using an Impact-Echo Method

Hailin Feng,[a] Yiming Fang,[a,*] Jian Li,[b] and Guanghui Li [b]

This paper presents a new methodology for detecting the longitudinal location of the hidden hole in a log using impact-echo testing. The hole and the end surface of the log produced two different amplitude peaks in the frequency spectrum after a mechanical tap on the top of the log. The ratio of the two frequencies was used to estimate the longitudinal position of the hole. The major advantage of this method is that it avoids measuring the travel velocity of the stress wave, which is sensitive to many factors and then poses a formidable challenge to the realization of inspection. Experimental studies were carried out using Pine logs with mechanically drilled holes and a *Cinnamomum camphora* log with natural hole. The results indicated that the estimated positions were in good agreement with the actual position of the hole. The impact-echo testing can be applied to detect the longitudinal position of the internal hole in log.

Keywords: Non-destructive testing; Log; Internal hole detection; Longitudinal position determination; Impact-echo testing

*Contact information: a: School of Information Engineering, Zhejiang A & F University, Hangzhou City, P. R. China; b: Zhejiang Provincial Key Laboratory of Forestry Intelligent Monitoring and Information Technology, Hangzhou City, P. R. China; *Corresponding author: ymfang@zafu.edu.cn*

INTRODUCTION

Wood is a valuable engineering material with a high strength to weight ratio and is widely used as a structural element. Holes in the wood, caused by insects, loose knots, cracks, or fungus, frequently lead to poor mechanical performance. Consequently, the hole should be detected before further use or processing of the wood. Visual inspection is the easiest and lowest cost method for log inspection if hole is present in the wood. However, this method is ineffective with hidden holes because there may be no external evidence of their presence. The desire for wood-based products in industry has driven extensive research to detect hidden hole in logs using a non-destructive method.

The acoustic technique has been attracting attention and developing rapidly (Roohnia *et al.* 2011; Sohi *et al.* 2011). In principle, different internal conditions, that is, sound, deterioration, or the decay of logs often result in a modified propagation velocity of the acoustic wave (Wang 2013). Hence, the flight time of the acoustic wave, together with the prior knowledge of the logs, provides internal information about the logs (Li *et al.* 2014). In our previous work, tomographic images were reconstructed from the time of flight (TOF) data with the implementation of the interpolation algorithm. Information concerning the size, shape, and position of the internal defect was presented in an intuitive manner (Feng *et al.* 2014). However, the described work mainly focused on the inspection of the cross-sectional modes. Therefore, these methods cannot be directly employed to estimate the longitudinal position of the internal hole in a log.

The impact-echo method is a popular technique for non-destructive testing. Stress waves are excited from a short duration mechanical impact. The frequency spectra obtained from the recorded waveforms are affected by the conditions of the test sample. Depending on the emerging amplitude peak in the frequency spectrum, the presence and location of internal defects can be determined. This approach has been widely employed to detect defects in many disciplines. It was revealed that the axisymmetric void, non-axisymmetric void, and neck could be detected in the frequency domain (Kim *et al.* 2002). Wang *et al*. (2012) evaluated Poisson's ratio using the materials: concrete, steel, stainless steel, and brass with the impact-echo testing method. Experimental data yielded satisfactory results. The work done by Kee *et al*. (2011) demonstrated that the impact-echo method is a practical option for consistent and rapid *in-situ* evaluation of reinforced concrete bridge decks.

However, until now, only a small number of successful applications in wood testing have been mentioned in the literature. Conventional impact-echo based methods depend upon knowledge of the propagation velocity of the stress wave, which presents a challenge to realize a precise testing of logs. In contrast to metal, wood is a complex, inhomogeneous material. The propagation of the stress wave is affected by many natural features, such as moisture content, knots, texture angle, earlywood, and latewood (Wang *et al.* 2004). It becomes very difficult to obtain an accurate value of the velocity. Thus, there is a strong need to investigate novel approach with which no prior information concerning velocity is required.

In this paper, a novel method is proposed aiming to eliminate the effects of travel velocity on the results of log inspection. Although the method is still based on the echo signals, a different system is used for processing the signals. Unlike conventional approaches, this method does not involve any determination of frequency displacements or travel time. More attention is paid to the changes in magnitude spectrum. Moreover, the travel speed of the stress wave is not involved in the computation. Accordingly, the detection is no longer affected by the inhomogeneity, anisotropy and natural variability of wood.

Principle of the Impact-Echo Method

The principle of the impact-echo method is illustrated in Fig. 1. When a hammer strikes the top of the log, a longitudinal stress wave (P wave) is introduced to the log and travels through the log. This wave will be reflected at the end of the log, whereupon it returns in the reverse direction. While being reflected several times, the recording is transmitted by a receiver sensor attached on the top of the log. Then, the obtained signal, which indicates the reverberation of the wave, is processed using Fast Fourier Transform (FFT). If an internal hole is present, the heterogeneities will result in internal interfaces. The stress wave will be reflected both on the interfaces of hole and the end of the log. Subsequently, additional peaks appear in the frequency spectra. By interpreting the change in the frequency domain, one can estimate the distance between the hole and the top, represented as d in Fig. 1. (Carino 2001; Yeh and Liu 2008)

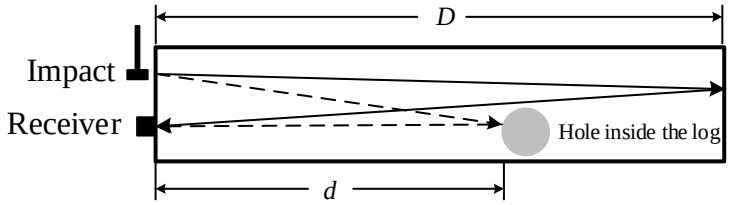

Fig. 1. Schematic illustration of the impact-echo technique

Frequency Spectrum of the Sound Log

Wang *et al*. (2003) suggested that a defect-free log can be treated as a cylindrical orthotropic form with a taper. The stress wave speed (C) in a log is dependent upon the longitudinal elastic modulus of the log (E_L) and the log's density (ρ) (Eq. 1):

$$C = \sqrt{\frac{E_L}{\rho}} \quad (1)$$

The n order resonance frequency f_n of the echo-wave can be expressed as follows (Lin 1997) (Eq. 2),

$$f_n = \frac{C}{2D}\left(n + \frac{1}{\pi} tg^{-1}\frac{KC}{2\pi f_n E_L S}\right), n = 1,2,3 \ldots \quad (2)$$

where S denotes the area of the cross section, D is the length, and K is the stiffness ratio (Lin 1997).

According to Newton's third law and the force balance relationship, K equals approximately zero (Liu 2012). Hence, a simpler approximation of f_n as follows is used (Eq. 3):

$$f_n = n\frac{C}{2D} \quad (3)$$

When n equals 1, the fundamental frequency f_1 can be achieved as follows:

$$f_1 = \frac{C}{2D} \quad (4)$$

Hole Location Determination with Spectra Analysis

When an internal hole is present, the stress wave is reflected on the surface of the hole beside the end surface of the log. The reverberations on the hole surface are shown in Fig. 1 with a dashed line. Then a new component is added to the received signal, and a new peak emerges in the magnitude spectrum. For convenience, the new peak frequency is defined as f_{h}. In principle, the period of the new component is two times of the travel time. The distance between the top of the log and the surface of the hole, as shown in Fig. 1, is defined as d. Hence, f_{h} can be determined by (Eq. 5):

$$f_h = \frac{C}{2d} \quad (5)$$

From Eq. 5, it can be inferred that the frequency f_h is relevant to the distance between the hole and the top of the log. Given the travel velocity *C*, the value of *d* can be calculated with the frequency f_h. Therefore, Eq. 5 has been widely used in impact-echo testing of homogeneous materials. However, such an approach does not work well in the inspection of wooden products. The travel velocity of stress wave, which plays key role in the calculation, is sensitive to microstructure and physical properties of wood. This sensitivity causes difficulties and lower precision in the impact-echo testing of log.

In this work, Eq. 5 is used indirectly aiming to avoid measurement of *C*. Generally, the wave travels at a constant speed in the same log. Combining Eqs. 4 and 5, the value of d can be estimated by using the ratio of f_1 to f_{h} (Eq. 6),

$$\hat{d} = \frac{D \cdot f_1}{f_h} \quad (6)$$

where $\hat{d}$ is the estimated value of d. From Fig. 1, it can be observed that the waves with frequency of f_1 travel longer before being reflected than those of f_h. This means that their periods are longer. Then f_h is definitely larger than f_1. Therefore the estimated $\hat{d}$ will be within the range from 0 to D.

In Eq. 6, f_1 should be the fundamental frequency of the defect-free log. In general, it is different from the fundamental frequency measured with a defective log because an internal hole consequently leads to a longer travel time of the stress wave (Wang 2013). However, for a given defective log, it is hard to obtain the corresponding fundamental frequency for the defect-free condition. In this work, the fundamental frequency obtained with the test sample was used as a substitute for the fundamental frequency of the sound log.

Note that what can be estimated using Eq. 6 is the distance between the top of the log and the nearest surface of the hole, as shown in Fig. 1. By conducting testing on the other side of the log, the distance between the end and the hole on the other side can also be obtained. Other information regarding longitudinal positions, such as geometrical center, can be determined with further calculations. For simplicity, this paper mainly focused on the testing at one side because of the similarity of the testing.

EXPERIMENTAL

Materials and Experimental Setup

Test specimen

Three pine logs, as shown in Fig. 2, were employed in this study, aiming to evaluate the performance of the method. They were numbered from 1 to 3 and the sizes were Φ 0.22 × 2.1 m (No. 1), Φ 0.25 × 2.0 m (No. 2), and Φ 0.25 × 2.1 m (No. 3).

Fig. 2. Photo of the pine logs

An acoustic tomography device provided by Fakkop Enterprise of Hungary was employed to remove the suspicion of having internal defects. With a few taps on each sensor evenly spaced along the log, acoustic images can be developed. Figure 3 shows the inspection results. In the images, three color schemes (green, red, and blue) were used to

represent the internal conditions of logs, which corresponded to "sound", "decayed", and "hollow", respectively. Obviously, the used logs were quite healthy because the images were dominated by green color.

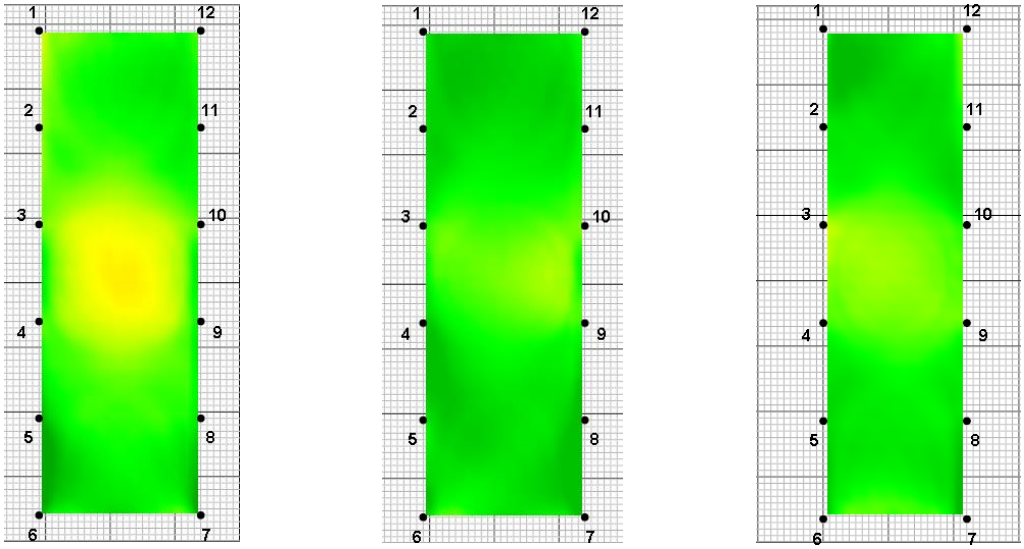

Fig. 3. Acoustic images of the pine logs developed by Fakkop tomography equipment: (a) Image of the No.1 log; (b) Image of the No.2 log; (c) Image of the No.3 log

A *Cinnamomum camphora* log, shown in Fig. 4(a), was also employed in this study, aiming to further evaluate the performance of the method. The size of the log was Φ 0.18 × 1.6 m. The visual inspection of the sample did not show any indication of there being a hole over the entire log. However, from Fig. 4(b), it can be seen that there existed an internal hole because a blue area appeared in the Fakkop image. The hole can also be located from Fig. 4(b). It was about 1.0 m apart from the A side of the log and 0.4 m from the B side.

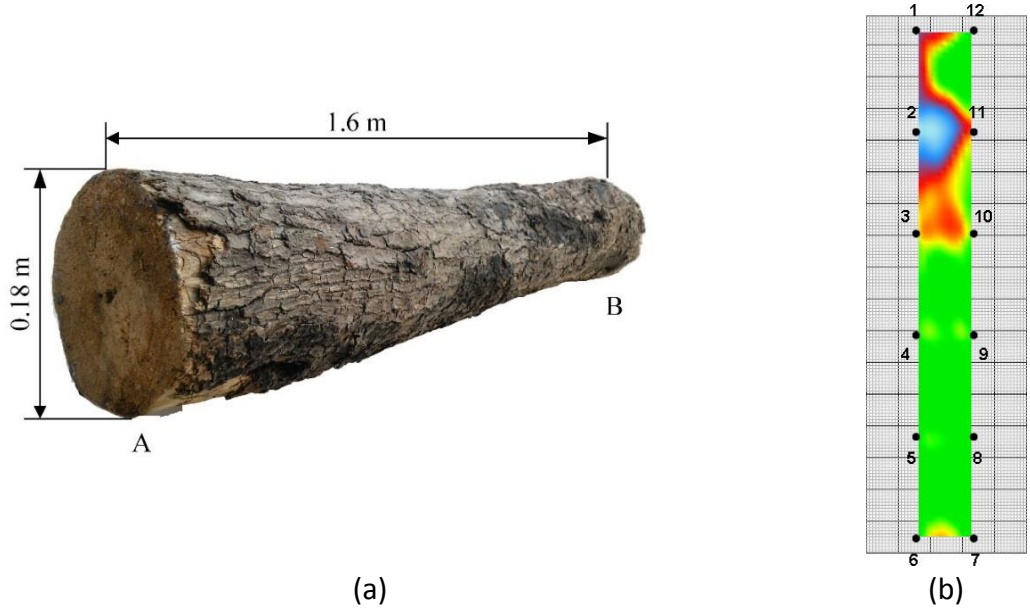

Fig. 4. The *Cinnamomum camphora* log used in this work: (a) Photo; (b) Fakkop image

Test apparatus

The piezoelectric sensor used in this work (Model: BZ1105) was from Beidaihe Institute of Electrical Automation, China. A digital oscilloscope (Model: TDS2022B) was from Tektronix Inc., United States and Matlab software. The piezoelectric sensor was attached to one side of the log to collect the echo-wave. Subsequently, the signal output from the sensor was measured by the oscilloscope. The sampling frequency was 100 KHz. Matlab was employed to compute the frequency spectra of the recorded signals.

Test procedures

Firstly, the experiments were conducted using the three defect-free pine logs without a hole. The A side of each log was struck with a hammer, as shown in Fig. 1. The striking point was 0.08 m apart from the pith center, and the piezoelectric sensor was deployed at 0.16 m from the striking point. After the experiments with the sound logs, several simulated holes were drilled into each log. Figure 5 illustrates the positions and sizes of the drill holes. The distance between the A side of the log and the nearest surface of the hole was 0.2 m in the No.1 log. In the other two logs, the distances were 0.6 m (No. 2) and 1.0 m (No. 3). The impact-echo testing began with a 0.05 × 0.10 m hole in each log. The smaller holes were expanded to make larger ones (0.10 × 0.20 m and 0.15 × 0.30 m) after the preceding testing had been completed.

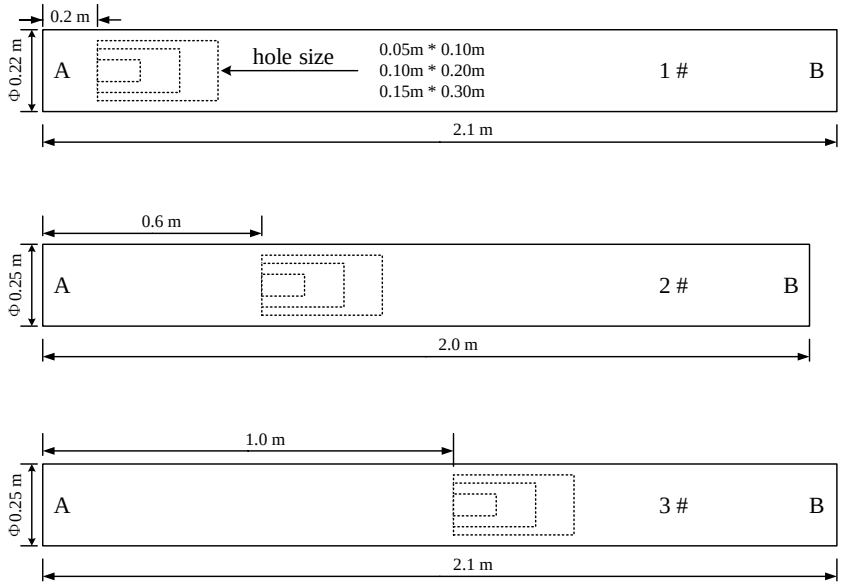

Fig. 5. Positions and sizes of the holes drilled into each log

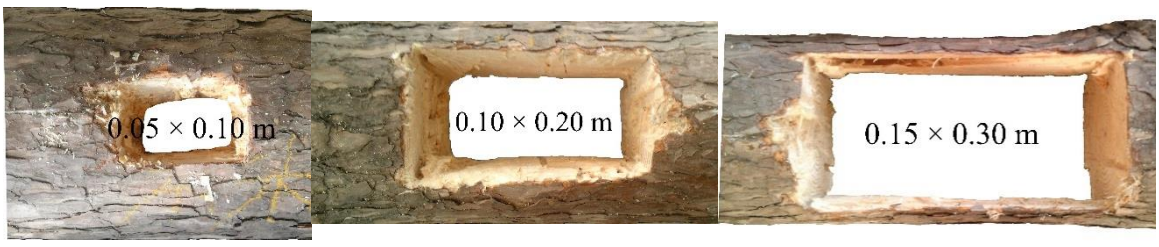

(a) (b) (c)

Fig. 6. Photos of simulated holes with different sizes: (a) 0.05×0.10 m; (b) 0.10×0.20 m; (c) 0.15×0.30 m

It is almost impossible to drill an internal hole while keeping the bark and the surface of the log intact. So the simulated holes we drilled in this study were visible and can be inspected with human eyes. Fig. 6 showed three typical holes.

Finally, the experiments were conducted on both A and B sides of the *Cinnamomum camphora* log displayed in Fig. 4, aiming to predict the presence and position of the natural defect.

Results and Analysis

Performance on simulated holes

Figure 7 shows the spectra of the echo-waves collected on the A side of the No.1 log. The waveform in Fig. 7 (a) corresponded to the defect-free logs. Figures 7 (a), (b), and (c) show the spectra corresponding to the logs with holes of 0.05 × 0.10 m, 0.10 × 0.20 m, and 0.15 × 0.30 m, respectively. For comparison purposes, the waveform amplitudes were normalized with respect to the maximum amplitude of the waveforms.

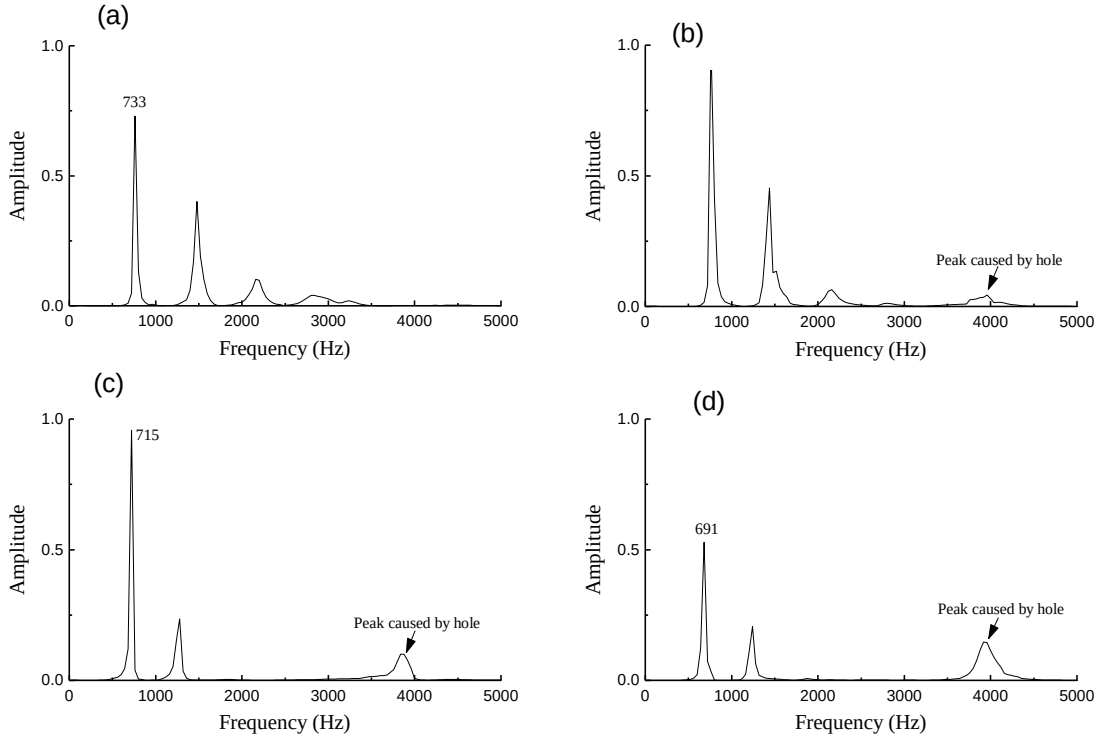

Fig. 7. Spectra of the echo-waves collected on the A side of the No.1 logs with (a) no drill hole, (b) drill hole of 0.05 x 0.10 m, (c) drill hole of 0.10 x 0.20 m, and (d) drill hole of 0.15 x 0.30 m

As mentioned above, four amplitude peaks can be observed in Fig. 7(a), and the frequencies increased linearly. They were the product of the fundamental frequency (f_1 = 733 Hz) and the order, n. This was in good agreement with Eq. 3. When the hole was present in the log, the spectrum changed accordingly. Compared with Fig. 7(a), there were emergent peaks around the frequency of 4000 Hz, as shown in Fig. 7(b), (c), and (d). Therefore, the stress waves reflected the presence of the hole in the log. According to Eq. 5, the frequency at the emerging peak can be referred to as f_h, which were 3960 Hz, 3840 Hz, and 3920 Hz respectively, as listed in Table 1. The same experiments were then conducted with the No. 2 and the No. 3 logs. The frequencies were also recorded in the same way as the above experiments.

Table 1. Frequencies Recorded in Experiments

Specimen	Hole size (m)	f_1 (Hz)	f_h (Hz)
No. 1	0.05 x 0.10	726	3960
	0.10 x 0.20	715	3840
	0.15 x 0.30	691	3920
No. 2	0.05 x 0.10	717	2472
	0.10 x 0.20	696	2442
	0.15 x 0.30	688	2596
No. 3	0.05 x 0.10	703	1491
	0.10 x 0.20	690	1525
	0.15 x 0.30	679	1584

Then, by applying Eq. 6 to the frequencies listed in Table 1, the longitudinal position of the hole ($\hat{d}$) were computed and are listed in Table 2. To evaluate the precision, the absolute error of the estimated position is also provided in Table 2. The absolute error (ε) was computed by (Eq. 7):

$$\varepsilon = \left| d - \hat{d} \right| \tag{7}$$

Table 2. Estimation Results using the Data listed in Table 1

Specimen	Hole size (m)	$\hat{d}$ (m)	d (m)	ε (m)
No. 1	0.05 x 0.10	0.385	0.2	0.185
	0.10 x 0.20	0.391		0.191
	0.15 x 0.30	0.370		0.170
No. 2	0.05 x 0.10	0.58	0.6	0.020
	0.10 x 0.20	0.57		0.030
	0.15 x 0.30	0.53		0.070
No. 3	0.05 x 0.10	0.99	1.0	0.010
	0.10 x 0.20	0.95		0.050
	0.15 x 0.30	0.90		0.100

The results indicated that the presented method was capable of determining the longitudinal position of the hole. Considering the No. 1 log, the estimated values of the positions, $\hat{d}$, were 0.385 m, 0.391 m, and 0.370 m when the hole sizes were 0.05 × 0.10 m, 0.10 × 0.20 m, and 0.15 × 0.30 m, respectively. If the hole was far from the top of the log, a precise estimation could be obtained. When the testing was conducted with the No.2 log, the estimation error decreased significantly. The ε were 0.02 m, 0.03 m and 0.07 m at the hole sizes of 0.05 × 0.10 m, 0.10 × 0.20 m, and 0.15 × 0.30 m, respectively, which were much lower values in comparison to the results of the No. 1 log. The same tendency can be observed in the results of the No. 3 log. The ε of the No. 3 log was 0.01 m, 0.05 m and 0.10 m, respectively, which implied a precise estimation of the longitudinal position of the drilled hole.

Performance on natural hole

Figure 8 shows the spectrum of the signal collected from the A side of the *Cinnamomum camphora* sample. It can be seen that there were three peaks at 1007 Hz, 1728 Hz, and 2005 Hz, respectively. Among the three frequencies, 1007 Hz was approximately half that of the other frequencies. Therefore, the authors concluded that the

frequency of 1007 Hz was the fundamental frequency f_1 and the frequency of 2005 Hz was the second order resonance frequency f_2. Hence, the frequency of 1728 Hz can be considered as f_h, which indicated the presence of a hole in the log. Finally, the distance between the A side and the hole (d) can be computed using Eq. 6. The value of $\hat{d}$ was 0.93 m.

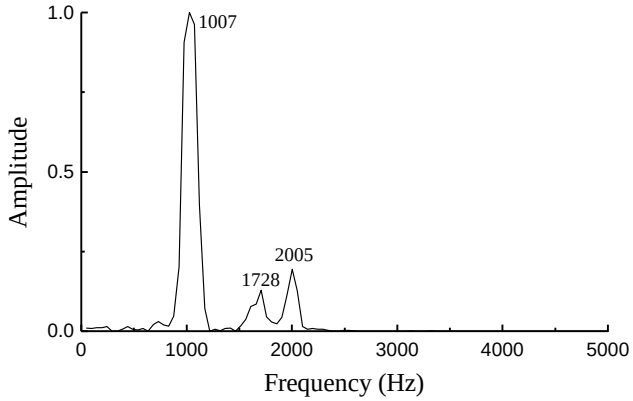

Fig. 8. Spectrum of the stress wave collected on the A side of the *Cinnamomum camphora* log

The same testing was conducted on the B side of the *Cinnamomum camphora* log, aiming to determine the distance between the hole and the B side. Figure 9 shows the obtained spectrum, which definitively displayed three amplitude peaks. These peaks are shown at 1025 Hz, 2001 Hz, and 4320 Hz. The frequency of 1025Hz was about half that of the 2001 Hz frequency peak. However, there were no linear relationships between the 4320 Hz and the other two frequencies. Thus, one can assume that the f_1 corresponded to the 1025 Hz and the f_h corresponded to the 4320 Hz frequencies. It was determined that a hidden hole existed in the sample. Further, the hole was positioned 0.38 m from the B side by using Eq. 6.

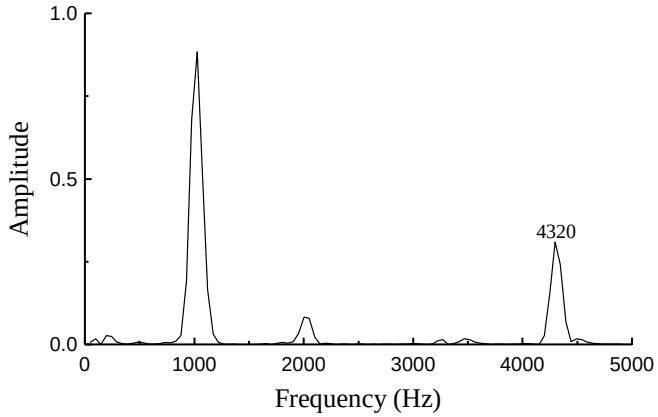

Fig. 9. Spectrum of the stress waves collected on the B side of the *Cinnamomum camphora* log

The experiments on the two sides indicated that the internal hole can be detected and the estimated positions were in good agreement with those displayed in Fig. 4(b). The errors of the estimated results from the two sides were 0.07 m and 0.02 m, respectively. After the impact-echo signals were analyzed, the log was cut to verify the results obtained. Figure 10 shows that there was an internal hole inside of the cross section. The hole was 1.0 m from the A side and 0.4 m from the B side. The effectiveness of the proposed method was verified again.

Fig. 10. Cross sectional area of the logs with the natural hole

CONCLUSIONS

1. Based on the spectra analysis, an internal hole is first detected, and then the longitudinal position of the hole is estimated using the ratio of two peak frequencies. Because the travel speed of the stress wave is not involved in the computation, the detection was no longer affected by the inhomogeneity, anisotropy, and natural variability of wood
2. A precise estimation can be achieved if the hole is not too near the top of the log. When the holes are 0.6 m and 1.0 m apart from the top, the estimation errors are significantly lower than that of the hole which is 0.2 m apart from the top.
3. The presented approach is believed to be applicable to a broad range of similar experiments, especially for the non-destructive testing of complex, inhomogeneous material. Further study is needed to confirm it.

ACKNOWLEDGMENTS

The authors are grateful for the support of the Natural Science Foundation of China (Grant. No. 61272313, 61302185, 61472368); the foundation from Zhejiang Provincial Science and Technology Department (Grant. No, LY15F020034, 2013C24026, 2013C31018, 2014C31044, LQ14F020014); Young academic leaders Foundation in Zhejiang Province (pd2013243).

REFERENCES CITED

Carino, N. J. (2001). "The impact-echo method: An overview," in: *Proceedings of the 2001 Structures Congress & Exposition*, American Society of Civil Engineers, Washington D.C., (http://vibrationdata.com/tutorials/impact_echo.pdf).

Feng, H. L., Li, G. H., Fu, S., and Wang, X. P. (2014). "Tomographic image reconstruction using an interpolation method for tree decay detection," *BioResources* 9(2), 3248-3263. DOI: 10.15376/biores.9.2.3248-3263

Kee, S. H., Oh, T., Popovics, J. S., Arndt, R. W., and Zhu, J. (2011). "Nondestructive bridge deck testing with air-coupled impact-echo and infrared thermography," *Journal of Bridge Engineering* 17(6), 928-939. DOI: 10.1061/(ASCE)BE.1943-5592.0000350

Kim, D. S., Kim, H. W., and Kim, W. C. (2002). "Parametric study on the impact-echo method using mock-up shafts," *NDT & E International* 35(8), 595-608. DOI: 10.1016/S0963-8695(02)00046-4

Li, G. H., Wang, X. P., Feng, H. L., Wiedenbeck, J., and Ross, R. J. (2014). "Analysis of wave velocity patterns in black cherry trees and its effect on internal decay detection," *Computers and Electronics in Agriculture* 104, 32-39. DOI: 10.1016/j.compag.2014.03.008

Lin, J. S. (1997). "Analysis of frequency domain curve in the reflection wave method of piling test," *South China Journal of Seismology* 17(3), 73-80.

Liu, J. S. (2012). "The application of elastic wave reflection method in the pile foundation inspection," *Advanced Materials Research* 594-597, 1109-1112. DOI: 10.4028/www.scientific.net/AMR.594-597.1109

Roohnia, M., Alavi-Tabar, S. E., Hossein, M. A., Tajdini, A., Jahan-Latibari, A., and Manouchehri, N. (2011). "Acoustic properties in Arizona cypress logs: A tool to select wood for sounding board," *BioResources* 6(1), 386-399. DOI: 10.15376/biores.6.1.386-399

Sohi, A. M. A., Khademi-Eslam, H., Hemmasi, A. H., Roohnia, M., and Talaiepour, M. (2011). "Nondestructive detection of the effect of drilling on acoustic performance of wood," *BioResources* 6(3), 2632-2646. DOI: 10.15376/biores.6.3. 2632-2646

Wang, J. J., Chang, T. P., Chen, B. T., and Wang, H. (2012). "Determination of Poisson's ratio of solid circular rods by impact-echo method," *Journal of Sound and Vibration* 331(5), 1059-1067. DOI:10.1016/j.jsv.2011.10.030

Wang, X. P. (2013). "Acoustic measurements on trees and logs: A review and analysis," Wood *Science and Technology* 47(5), 965-975. DOI: 10.1007/s00226-013-0552-9

Wang, X. P., Ross, R. J., Brashaw, B. K., Punches, J., Erickson, J. R., Forsman, J. W., and Pellerin, R. E. (2003). "Diameter effect on stress-wave evaluation of modulus of elasticity of logs," in: *Proceedings of the 13th International Symposium on Nondestructive Testing of Wood*, University of California, Berkley Campus California, USA, pp. 149-156, (http://www.treesearch.fs.fed.us/pubs/9119).

Wang, X. P., Ross, R. J., Green, D. W., Brashaw, B., Englund, K., and Wolcott, M. (2004). "Stress wave sorting of red maple logs for structural quality," *Wood Science and Technology* 37(6), 531-537. DOI: 10.1007/s00226-003-0202-8

Yeh, P. L. and Liu, P. L. (2008). "Application of the wavelet transform and the enhanced Fourier spectrum in the impact echo test," *NDT & E International* 41(5), 382-394. DOI: 10.1016/j.ndteint.2008.01.002

Article submitted: May 13, 2015; Peer review completed: June 22, 2015; Revised version received: September 12, 2015; Accepted: September 15, 2015; Published: September 23, 2015.
DOI: 10.15376/biores.10.4.7569-7579